



Design and preparation of HPW-anchored magnetic carbon nitride nanosheets: an efficient and eco-friendly nanocomposite for one-pot synthesis of α -amino phosphonates

Asieh Azhdari¹ · Najmedin Azizi^{1,2}

Received: 13 May 2021 / Accepted: 15 July 2021
© The Author(s), under exclusive licence to Springer Nature B.V. 2021

Abstract

Heterogeneous catalysis is one of the fastest and greatest developing branches and longstanding challenges in academic researchers and the chemical industry. Carbon-based material with various functional groups, the most abundant elements, and the main component in natural products provide a unique platform for heterogeneous catalysis due to their excellent biocompatibility and high performance. Herein, we introduce a novel nanocomposite comprising of different acids anchored to magnetic mesoporous carbon nitrides through a grindstone method to enhance nanocomposite catalysts' environmentally benign capability. As a result, the obtained porous magnetic catalysts show the highest possible activity and product selectivity for facile preparation of α -amino phosphonates derivatives in good to excellent yields at ambient temperature. This fast and straightforward methodology offers pot economy for the satisfactory reaction of various aldehyde, amine, and triaryl and trialkyl phosphite with a broad range of functional groups in a gram scale under mild reaction conditions.

Keywords α -Amino phosphonate · g-C₃N₄ · Phosphotungstic acid · Kabachnik–fields condensation · Magnetic carbon nitride nanocomposite

Introduction

Structural varieties of carbon compounds, namely activated carbon, graphite, graphene, nanotube, and carbon nitride, have outstanding physicochemical, thermal, and electrical properties. Their various applications as supports or catalysts are

✉ Najmedin Azizi
azizi@ccerci.ac.ir

¹ Department of Chemistry, Islamic Azad University, Ahvaz Branch, Ahvaz, Iran

² Chemistry & Chemical Engineering Research Center of Iran, P.O. Box 14335-186, Tehran, Iran

becoming more prominent, as evidenced by recent literature reports in this area [1–3]. Graphitic carbon nitride ($g\text{-C}_3\text{N}_4$) are usually considered the most appealing and attractive carbon-based polymers, with unique physicochemical properties such as excellent chemical stability, controllable chemical composition, and economic benefits [4–6]. Due to these unique properties, $g\text{-C}_3\text{N}_4$ porous polymers have been widely used in the artificial photosynthesis, adsorbents, sensors, and visible photocatalysis field in recent years [7–9]. However, a common issue in the practical application of bulk $g\text{-C}_3\text{N}_4$ is their unsatisfactory catalytic activity due to the insufficient functional groups on the polymer's surface. On the other hand, scalable and straightforward functionalization/modification strategy in the $g\text{-C}_3\text{N}_4$ surface because of the rigid template is difficult hardly possible [6, 10–15]. In this context, tremendous research and extensive investigations have been reported on the functional modifications of $g\text{-C}_3\text{N}_4$ using exfoliation, doping, and hybridizing to enhance catalytic performance [16–27]. On the other hand, there is no report on the $g\text{-C}_3\text{N}_4$ nanocomposite preparation via mechanical grinding in the literature. Herein, we fabricated $g\text{-C}_3\text{N}_4$ nanocomposite with different Lewis and Bronsted acid in a more straightforward manner and were explored for the greener production of α -amino phosphonates.

Phosphonates and phosphonic acids are highly stable phosphorus-containing compounds and play an essential role in the cell's physiological activity [28–30]. α -Aminophosphonates are privileged compounds in the design of pharmaceutically active compounds and valuable building blocks in constructing organophosphate pesticides, dyes, and functional materials [31]. Furthermore, α -amino phosphonates find extensive use as an anticancer, antibacterial, antitumor drug, plant growth regulator, and enzyme inhibitor [32, 33].

Arbuzov discovered alkyl phosphonates in 1906 [34, 35], and subsequently, Osipova made *N*-alkoxy α -amino phosphonates from the reaction of trimethyl phosphite and oxime. Among different approaches to forming α -amino phosphonates, the Kabachnik–Fields and aza-Pudovik reactions have been accepted as convenient and essential routes in the literature. The Kabachnik–Fields reaction was the most extensively studied as an excellent mild method that affords α -amino phosphonates in acceptable yields with the catalyst system's proper choice. In this context, many catalysts, including ionic liquids, nanocatalysts, metal catalysts, commercial Bronsted, and Lewis acid, organic functionalized polymers, have been devoted to promoting its reactions [36–39]. Among the reported methods, the nucleophilic addition of dimethyl phosphite and trimethyl phosphite to iminium salts or imines is more convenient. Imine formation was very rapid and straightforward and usually activated both acidic and basic media. However, in these approaches, the catalyst is used in over stoichiometric quantities. The procedures frequently requested a purification step and less satisfactory from the perspective of chemical efficiency and eco-friendliness. The substrate scope is limited to a few raw materials, particularly trialkyl phosphites, typically considered superior nucleophiles [40–42].

In recent years, our research has been interested in designing a new eco-friendly system using environmentally friendly solvents and benign catalysts in organic transformations [43–46]. Herein, we report a straightforward and fast preparation of aryl/

alkyl α -amino phosphonates by one-pot reaction of carbonyl compounds, amines, and phosphite derivatives promoted by magnetic carbon nitride nanocomposite.

Experimental

Chemicals and reagents

All commercial reagents and solvents were supplied from Merck, Germany, and used as received. The ^1H and ^{13}C NMR spectra were recorded by a Bruker Avance (500 MHz for ^1H and 125 MHz for ^{13}C). $\text{H}_3\text{PW}_{12}\text{O}_{40}$ was purchased from Aldrich. Fe_3O_4 and $\text{g-C}_3\text{N}_4$ were synthesized according to our previous work [23]. Melting points were recorded on a Buchi R-535 apparatus.

General procedure for the preparation of $\text{g-C}_3\text{N}_4$

Bulk $\text{g-C}_3\text{N}_4$ was by a facile thermal treatment of melamine source [23]. In brief, 10 g of melamine was heated at 550 °C for 3 h at a ramp rate of 5 °C/min. The $\text{g-C}_3\text{N}_4$ nanosheets were exfoliated from bulk $\text{g-C}_3\text{N}_4$ under air.

Fabrication of $\text{HPW@Fe}_3\text{O}_4/\text{g-C}_3\text{N}_4$ nanocomposite

0.7 g C_3N_4 and 0.3 g Fe_3O_4 were ground in mortar for 3 min. After that, 0.3 g phosphor tungstic acid ($\text{H}_3\text{PW}_{12}\text{O}_{40} = \text{HPW}$) was added and ground by mortar until produced black powder of $\text{HPW@Fe}_3\text{O}_4/\text{g-C}_3\text{N}_4$.

General procedure for the preparations of α -amino phosphonates

In a test tube with a mechanical stirrer, aniline (0.5 mmol), benzaldehyde (0.5 mmol), triphenyl, or trialkyl phosphite (0.5 mmol), $\text{HPW@Fe}_3\text{O}_4/\text{g-C}_3\text{N}_4$ (10 mg), and ethanol (1 mL) were added. The mixture was stirred at room temperature for 60 min until completion (followed by TLC analysis of reaction aliquots) then 10 mL of ethyl acetate was introduced. The magnetic nanocomposite was separated with an external magnet and washed with ethyl acetate and applied for the next runs. Recrystallization of the mother liquor to afford the α -amino phosphonates derivatives as pure products.

Result and discussion

The $\text{HPW@Fe}_3\text{O}_4/\text{g-C}_3\text{N}_4$ nanocomposite has been successfully prepared in two steps. This straightforward two-step process involves syntheses of the $\text{g-C}_3\text{N}_4$ nanosheet support and grafting Fe_3O_4 and HPW over the layers of $\text{g-C}_3\text{N}_4$, respectively. The surface morphologies of the resulting $\text{HPW@Fe}_3\text{O}_4/\text{g-C}_3\text{N}_4$ nanocomposites were investigated by scanning electron microscope (SEM). The SEM

analysis is depicted in Fig. 1. The SEM image of HPW@Fe₃O₄/g-C₃N₄ nanocomposite showed small sheet-like nanoparticles with holes on the g-C₃N₄. Furthermore, it can be observed that Fe₃O₄ and HPW nearly spherical or slightly irregular structures with small particles attached to the sheet layer of g-C₃N₄.

The energy-dispersive X-ray spectra (EDS) of HPW@Fe₃O₄/g-C₃N₄ are presented in Fig. 2. It can be seen in Fig. 2 that the presence of P, W, O, C, and N elements, implying that the HPW and Fe₃O₄ are uniformly coated on the g-C₃N₄ surfaces.

The Fourier transformed infrared spectroscopy (FTIR) also confirmed functional groups of the HPW@Fe₃O₄/g-C₃N₄ nanocomposite (Fig. 3). The characteristic peaks were shown at 1235.34, 1320.52, 1408.78, 1634, and 804.92 cm⁻¹ for typical vibrations of heptazine-based molecular units of C=N and C-N in g-C₃N₄. FT-IR peaks at 3432 cm⁻¹ correspond to the N-H and NH₂ groups of g-C₃N₄ and the O-H groups due to the adsorption of water from the environments. The peak was shown

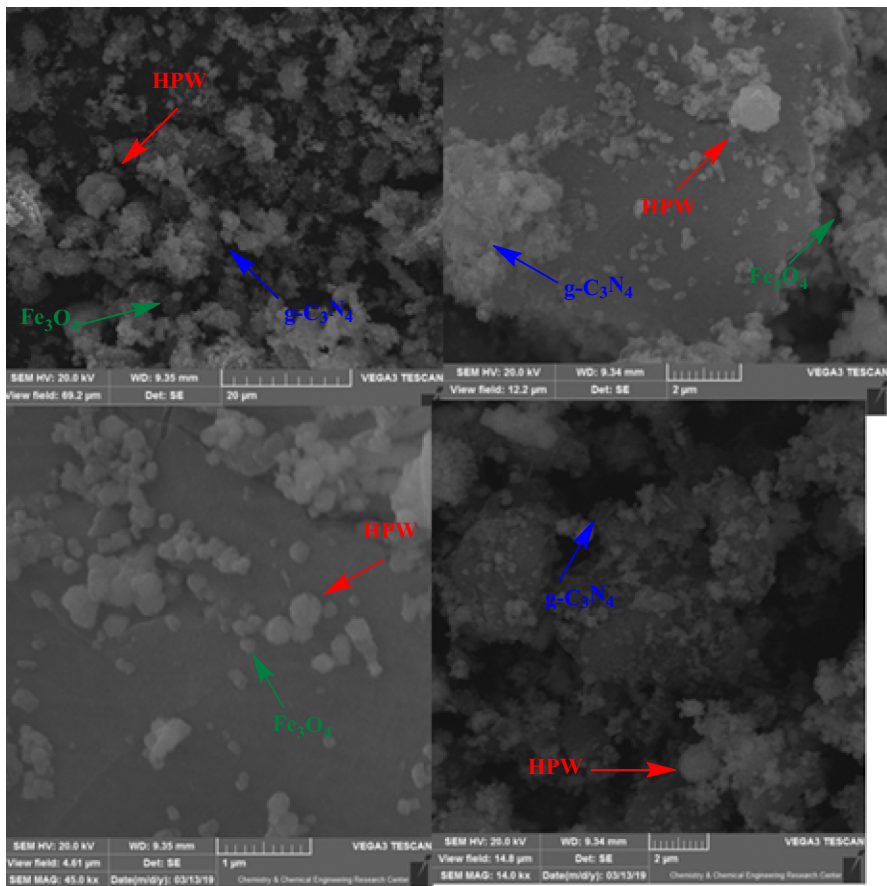


Fig. 1 SEM of HPW@Fe₃O₄/g-C₃N₄ nanocomposite

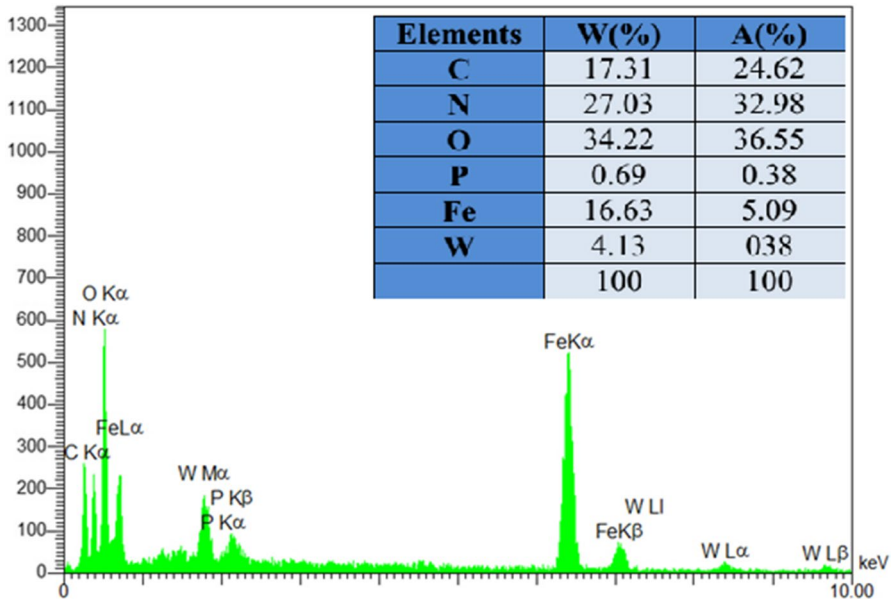


Fig. 2 EDX analysis of HPW@Fe₃O₄/g-C₃N₄ nanocomposite

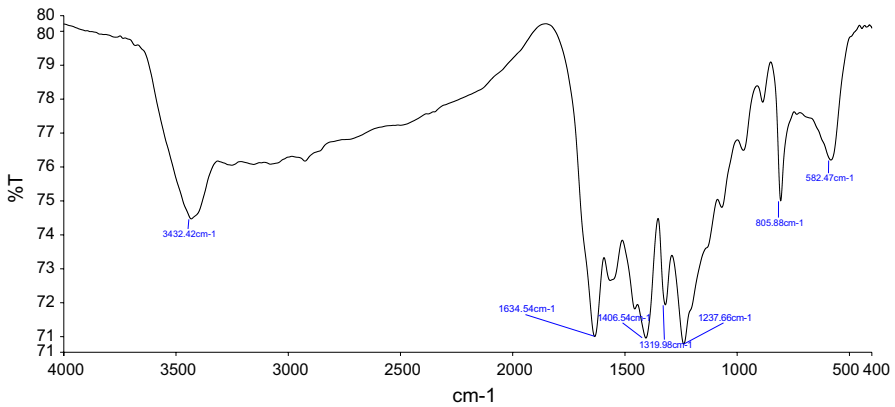


Fig. 3 FT-IR spectra of HPW@Fe₃O₄/g-C₃N₄ nanocomposite

at 582 cm⁻¹ for Fe₃O₄. The peak was shown at 950 cm⁻¹ cm for P–O and the peaks were shown at 691 and 805 cm⁻¹ for W–O in phosphotungstic acid.

To further analyze the surface composition and structure of HPW@Fe₃O₄/g-C₃N₄, XRD analysis was carried out (Fig. 4).The XRD pattern of HPW@Fe₃O₄/g-C₃N₄ conforms structure of the g-C₃N₄, phosphotungstic acid, and Fe₃O₄. As shown in Fig. 4, six reflections are observed in the XRD pattern of Fe₃O₄ 31.19, 35.43, 44.7, 53.27, 57.03 and 62.6° that belong to the (2 2 0), (3 1 1), (4 0 0), (4 2 2), (5 1 1) and (4 4 0) plane diffractions of Fe₃O₄, in addition to the observed reflections

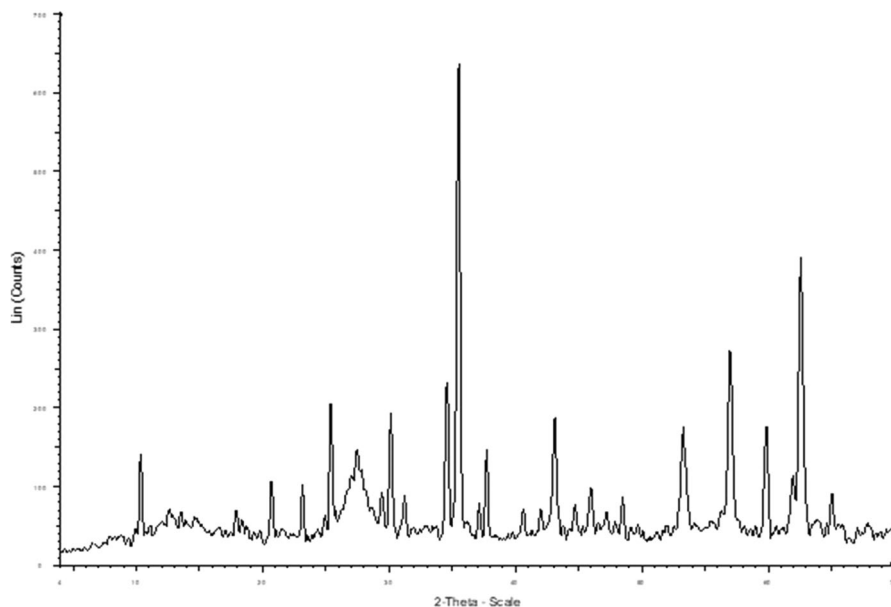


Fig. 4 The XRD spectra of HPW@Fe₃O₄/g-C₃N₄ nanocomposite

at 23.11, 24.85, 25.3 and 34.52 that belong to the (0 0 2), (0 2 0), (2 0 0) and (2 0 2) plane diffractions of WO₃. Furthermore, seven six reflections are observed in 29.39, 37.1, 40.6, 44.7, 47.88, 49.6 and 57.03° that belong to the (2 0 1), (1 0 5), (1 0 7), (2 0 7), (2 0 6), (3 0 4) and (3 1 4) plane diffractions of PO₄. The two characteristic peaks at 13.1 and 27.4° identified the typical layered C–N structure of g-C₃N₄.

Figure 5 shows a typical magnetization curve of HPW@Fe₃O₄/g-C₃N₄ nanocomposite and Fe₃O₄ nanoparticles at room temperature. The magnetization of the composite was entirely saturated at high fields and the saturation magnetizations of pure Fe₃O₄ and HPW@Fe₃O₄/g-C₃N₄ were 42.5 and 24.6 emu/g, respectively. Due to the functionalization by HPW and g-C₃N₄, the decrease in the saturation magnetization of composite, compared with pure Fe₃O₄ was observed. The strong magnetization of the composite can completely meet the requirement of the magnetic separation from the reaction system with an external magnet.

The synthesized nanocomposite catalytic activity was evaluated by synthesizing α -(phenylamino) benzyl phosphonates in the model system to adjust the reaction parameters (Table 1). In the model system, aniline (0.5 mmol), benzaldehyde (0.5 mmol) and triphenyl phosphite (0.5 mmol), ethanol (1 mL), and various kinds of g-C₃N₄-based catalyst were added. When the reaction was performed in the absence of catalyst for 80 min at room temperature, it was found that only 13% yield and the starting materials along with imine intermediate were recovered. Subsequently, a broad diversity of g-C₃N₄ derivatives was synthesized to study their activity in the preparation of α -(phenylamino) benzyl phosphonates. Among several kinds of g-C₃N₄ nanocomposites, HPW@Fe₃O₄/g-C₃N₄ (Table 1, entry 14) was the most effective catalyst since it resulted in the highest

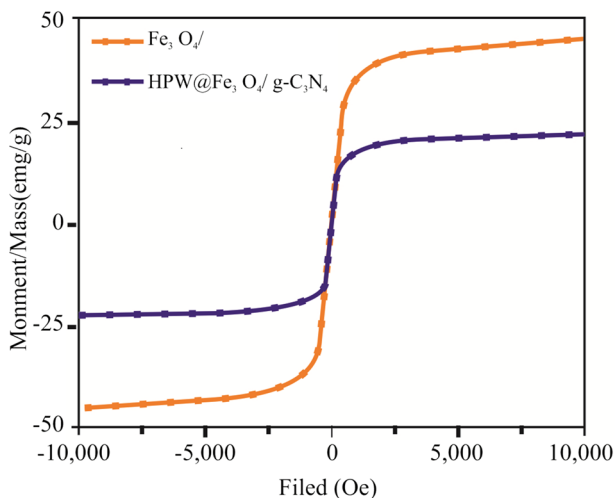


Fig. 5 VSM result of Fe_3O_4 and $\text{HPW}@Fe_3O_4/g-C_3N_4$

transformation to the desired phosphonate 4a. The catalytic performance of nanocomposite elements, namely $g-C_3N_4$, Fe_3O_4 , and HPW, was also examined. The results showed that nanocomposite elements were able to promote the model reaction in moderate yields (Table 1, entries 8–10 and 23–25). The results manifested that 10 mg of the composite was suitable to catalyze the model reaction in excellent yields (Table 1, entry 14) and a higher amount of composite (30, 50 mg) did not have notable effect on the model reaction (Table 1, entry 15, 16). Various protic and aprotic organic solvents were first examined. The results showed that ethanol was the most favorable media (Table 1, entries 14) among the tested solvents (Table 1, entries 18–22). The model reaction was ultimately best carried out using 0.5 mmol of aniline, 0.5 mmol of benzaldehyde, 0.5 mmol of triphenyl phosphite, and 10 mg of nanocomposite in ethanol for 60 min at room temperature (Table 1, entry 14).

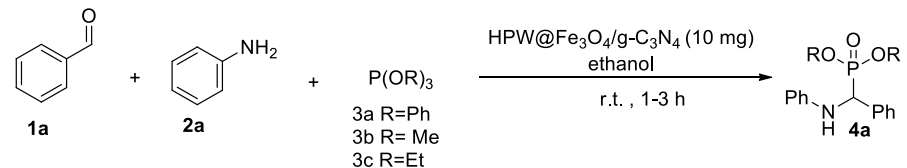
After determining the optimized condition, various reactions using aniline derivatives and aliphatic/aromatic carbonyl compounds with trialkyl/triphenyl phosphite in the presence of 10 mg of $\text{HPW}@Fe_3O_4/g-C_3N_4$ were performed to identify generalities and limitations of the procedure (Table 2). The one-pot synthesis of α -amino phosphonates derivatives was succeeded from the reaction of various aromatic aldehydes, aniline derivatives, and phosphite sources in good to excellent yields. The reactions proceeded under mild conditions with a low reusable catalyst loading in a simpler manner. A range of aniline derivatives with electron-withdrawing groups and electron-donating groups underwent a one-pot reaction with aromatic aldehydes, affording various aryl and alkyl phosphonates at room temperature under short reaction times (Table 2).

The survey of Table 2 was shown us when electron-withdrawing groups on benzaldehyde (Table 2, entries 3, 5, and 7), the yield was increased and when electron-donating groups on benzaldehyde (Table 2, entries 2 and 4), the yield was decreased.

Table 1 Synthesis of α -(phenylamino) benzyl phosphonates in the model conditions

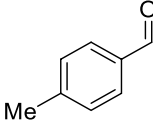
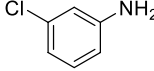
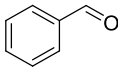
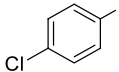
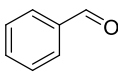
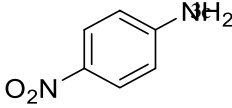
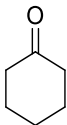
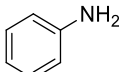
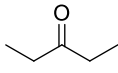
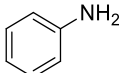
Entry	Catalysts	Amount of catalyst (mg)	time (min)	Solvent	Temp. (°C)	Yield (%)
1	Without catalyst	–	80	Ethanol	25	13
2	g-C ₃ N ₄	30	80	Ethanol	25	28
3	H ₂ SO ₄ @g-C ₃ N ₄	30	80	Ethanol	25	14
4	HCl@g-C ₃ N ₄	30	80	Ethanol	25	47
5	NH ₂ SO ₃ H@g-C ₃ N ₄	30	80	Ethanol	25	42
6	Basic Al ₂ O ₃ @g-C ₃ N ₄	30	80	Ethanol	25	53
7	CF ₃ COOH@g-C ₃ N ₄	30	80	Ethanol	25	61
8	Fe ₃ O ₄ /g-C ₃ N ₄	30	80	Ethanol	25	31
9	HPW/g-C ₃ N ₄	30	80	Ethanol	25	73
10	HPW@Fe ₃ O ₄	30	80	Ethanol	25	64
11	Fe ₃ O ₄ /ZnCl ₂ @g-C ₃ N ₄	30	80	Ethanol	25	79
12	Fe ₃ O ₄ /NiCl ₂ @g-C ₃ N ₄	30	80	Ethanol	25	78
13	Fe ₃ O ₄ /WCl ₆ @g-C ₃ N ₄	30	80	Ethanol	25	80
14	HPW@Fe ₃ O ₄ /g-C ₃ N ₄	10	80	Ethanol	25	94
15	HPW@Fe ₃ O ₄ /g-C ₃ N ₄	30	80	Ethanol	25	85
16	HPW@Fe ₃ O ₄ /g-C ₃ N ₄	50	80	Ethanol	25	82
17	HPW@Fe ₃ O ₄ /g-C ₃ N ₄	10	60	Ethanol	60	94
18	HPW@Fe ₃ O ₄ /g-C ₃ N ₄	10	60	Methanol	25	82
19	HPW@Fe ₃ O ₄ /g-C ₃ N ₄	10	60	Acetonitrile	25	78
20	HPW@Fe ₃ O ₄ /g-C ₃ N ₄	10	60	Ethyl acetate	25	76
21	HPW@Fe ₃ O ₄ /g-C ₃ N ₄	10	60	H ₂ O	25	74
22	HPW@Fe ₃ O ₄ /g-C ₃ N ₄	10	60	THF	25	79
23	g-C ₃ N ₄	10	60	Ethanol	25	20
24	Fe ₃ O ₄	10	60	Ethanol	25	28
25	HPW	10	60	Ethanol	25	45

When cyclohexanone and acetophenone as carbonyl groups were investigated in the model reaction, no conversion was observed (Table 2, entries 13, 14). To ensure this inception, two competition reactions denoted: (1) reaction between 0.5 mmol benzaldehyde, 0.5 mmol cyclohexanone, 0.5 mmol anilines, and 0.5 mmol triphenyl phosphite, (2) reaction between 0.5 mmol benzaldehyde, 0.5 cyclohexanone, 1 mmol aniline, and 1 mmol triphenyl phosphite. The investigation in reaction results has shown that cyclohexanone would not react, and it is related to the chemoselectivity of the reaction.

Table 2 Synthesis of α -(phenylamino) benzyl phosphonate derivatives by HPW@Fe₃O₄/g-C₃N₄ nano-catalyst

Entry	Benzaldehyde	Aniline	Phosphite	Yield (%)	M.P Found Rep	References
1			3a	94	142–144; 144–146 ³⁰	[30]
2			3b	91	148–150; 150–151 ⁴⁸	[48]
3			3a	93	160–162; 158–159 ³⁰	[30]
4			3c	91	125–126; 126–127 ⁴⁸	[48]
5			3b	95	133–135; 135–136 ³⁴	[34]
6			3b	92	163–164; 164–166 ³⁸	[38]
7			3a	94	130–131; 130–131 ⁴⁸	[48]
8			3c	92	66–67; 64–65 ³¹	[31]
9			3b	93	91–93; 92.5–94.5 ²⁸	[28]

Table 2 (continued)

Entry	Benzaldehyde	Aniline	Phosphite	Yield (%)	M.P Found Rep	References
10			3c	87	129–130: 128 ³⁸	[38]
11			3b	90	90–92: 88–90 ³⁸	[38]
12			3b	69	122–124: 124–126 ³⁸	[38]
13			3a	Trace	–	
14			3a	Trace	–	

Based on the above results, a plausible reaction mechanism of the Kabachnik–Fields reaction in the presence of HPW@Fe₃O₄/g-C₃N₄ nanocomposite is shown in Fig. 6. Initially, the carbonyl group of the aldehyde is activated by the nanocatalyst to react with the amine to form the imine product [1]. In the next step, the phosphite nucleophile is added to the resultant activated imine by the HPW supported on the g-C₃N₄ to give phosphonium intermediate [2] which then undergoes reaction with water to give α-amino phosphonates (Fig. 6).

The reusability of HPW@Fe₃O₄/g-C₃N₄ for the synthesis of α-(phenylamino) benzyl phosphonate was also investigated. After completing the reaction, the magnetic catalyst was removed with an external magnetic field and washed with ethanol and ethyl acetate. Subsequently, the catalyst was dried at 60 °C under vacuum and applied to the five successive runs without any significant change in the catalytic efficiency (Fig. 7). The heterogeneity of the nanocomposite was studied by XRD and EDS spectroscopy, representing that there is virtually no HPW-leaching (Figs. 8, 9).

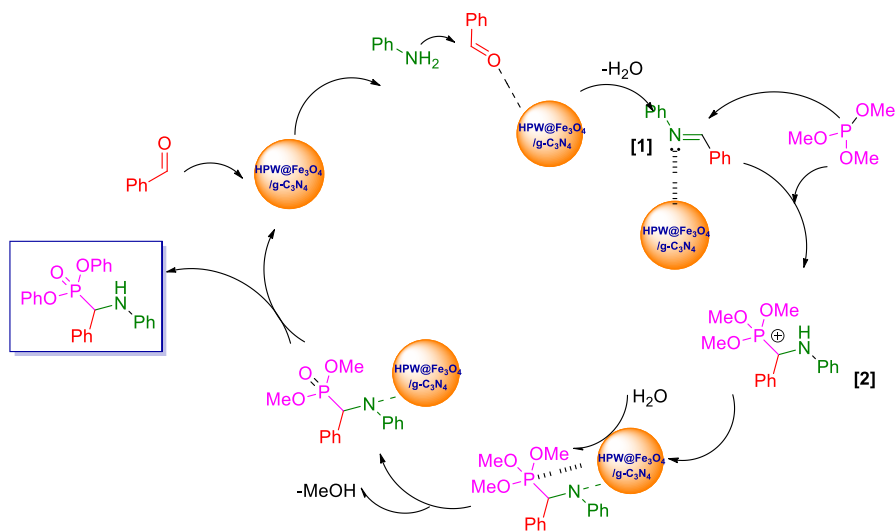


Fig. 6 The proposed mechanism of the Kabachnik–Fields reaction in the presence of $\text{HPW}@Fe_3O_4/g-C_3N_4$ nanocomposite

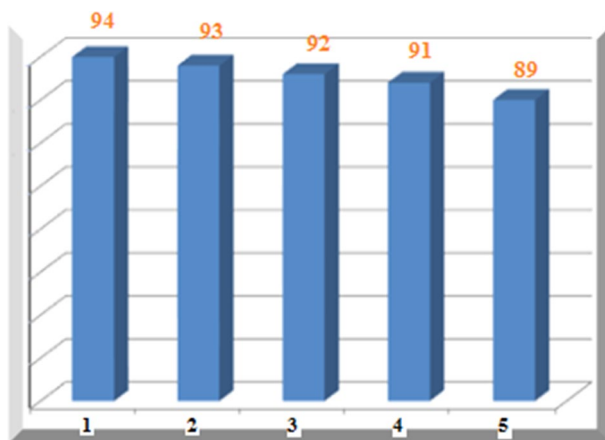


Fig. 7 Recyclability of $\text{HPW}@Fe_3O_4/g-C_3N_4$ nanocatalyst for synthesis of α -(phenylamino) benzyl phosphonate

Conclusion

In summary, an environmentally friendly magnetic carbon nitride catalyst, namely $\text{HPW}@Fe_3O_4/g-C_3N_4$ nanocomposite, was prepared by immobilization of HPW and Fe_3O_4 onto the $g-C_3N_4$ by grinding methods. By using this magnetic nanocomposite, the high-yielding three-component Kabachnik–Fields reaction was successfully achieved. This method provides notable advantages such as

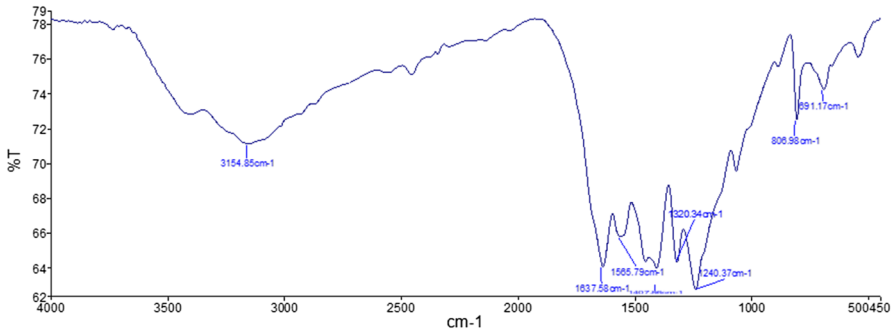


Fig. 8 FT-IR spectra of reused HPW@Fe₃O₄/g-C₃N₄ nanocomposite

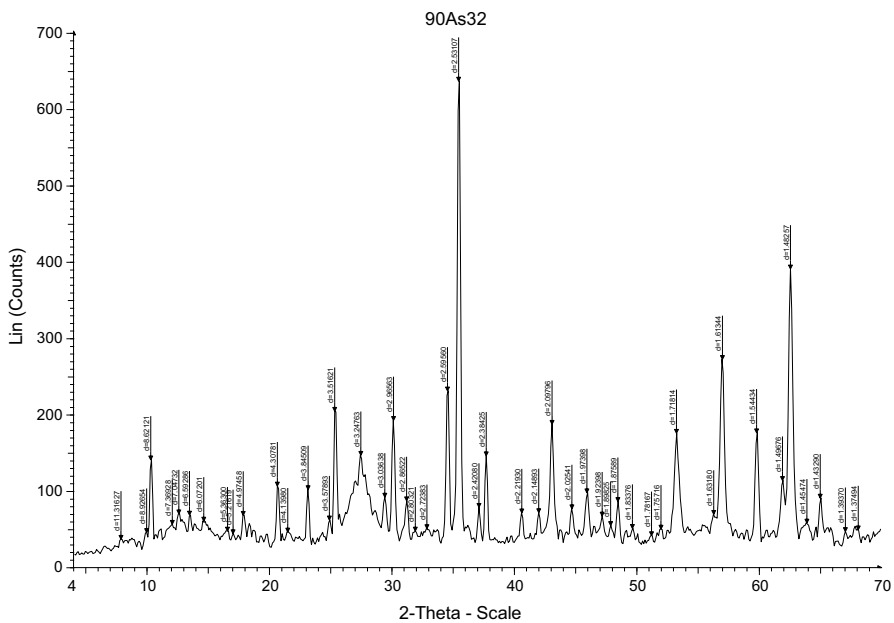


Fig. 9 The XRD spectra of reused HPW@Fe₃O₄/g-C₃N₄ nanocomposite

easy product separation and purification, excellent yields, short reaction times, a small amount of the catalyst. The magnetic catalyst could be separated easily and reused without a noticeable loss of catalytic activity.

Acknowledgements Financial support of this work by the Chemistry and Chemical Engineering Research Center of Iran is gratefully appreciated.

References

1. Z. Zhao, Y. Sun, F. Dong, *Nanoscale* **7**, 15 (2015)
2. Q. Han, N. Chen, J. Zhang, L. Qu, *Mater. Horiz.* **4**, 832 (2017)
3. Q. Liang, X. Liu, J. Wang, Y. Liu, Z. Liu, L. Tang, B. Shao, W. Zhang, S.H. Gong, M. Cheng, Q. He, C.H. Feng, *J Hazard Mater* **401**, 123355 (2021)
4. Y. Wang, X. Wang, M. Antonietti, *Angew. Chem. Int. Ed.* **51**, 68 (2012)
5. G. Liao, F. He, Q. Li, L. Zhong, R. Zhao, H. Che, H. Gao, B. Fang, *Prog. Mater. Sci.* **112**, 100666 (2020)
6. L. Chena, D. Zhua, J. Lia, X. Wanga, J. Zhub, P.S. Francis, Y. Zheng, *Appl. Catal. B.* **273**, 119050 (2020)
7. J. Zhu, P. Xiao, H. Li, S.A.C. Carabineiro, A.C.S. *Appl. Mater. Interfaces* **6**, 16449 (2014)
8. A. Wang, C. Wang, L. Fu, W. Wong-Ng, Y. Lan, *Nano-Micro Lett.* **47**, 1 (2017)
9. Y. Kong, C. Lv, C. Zhang, G. Chen, *Appl. Surf. Sci.* **515**, 146009 (2020)
10. Y. Zheng, J. Liu, J. Liang, M. Jaroniecc, S.Z. Qiao, *Energy Environ. Sci.* **5**, 6717 (2012)
11. A. Thomas, A. Fischer, F. Goettmann, M. Antonietti, J.O. Muller, R. Schlogl, J.M. Carlsson, *J. Mater. Chem.* **18**, 4893 (2008)
12. S. Yang, Q. Sun, Y. Shen, Y. Hong, X. Tu, Y. Chen, H. Zheng, *Appl. Surf. Sci.* **525**, 146559 (2020)
13. K. Yan, C. Mu, L. Meng, Z. Fei, P.J. Dyson, *Nanoscale Adv.* **3**, 3708 (2021)
14. S. Raha, M. Ahmaruzzaman, *Chem. Eng. J.* **395**, 124969 (2020)
15. M. Zulqarnain, A. Shah, M. Abdullah Khan, F.J. Iftikhar, J. Nisar, *Sci. Rep.* **10**: 6328 (2020)
16. Y. Han, M. Zhang, Y.Q. Zhang, Z.H. Zhang, *Green Chem.* **20**, 4891 (2018)
17. S. Cao, J. Yu, *J. Phys. Chem. Lett.* **5**, 2101 (2014)
18. T. Soleymani Ahoovie, N. Azizi, I. Yavari, M. Mahmoudi Hashemi, *J. Iran Chem. Soc.* **15**: 855 (2018)
19. T.S. Miller, A. Belen Jorge, T.M. Suter, A. Sella, F. Cora, P.F. McMillan, *Phys. Chem. Chem. Phys.* **19**, 15613 (2017)
20. L. Zhang, J. Zhang, J. Ma, D.J. Cheng, B. Tan, *J. Am. Chem. Soc.* **139**, 1714 (2017)
21. G. Dong, Y. Zhang, Q. Pan, J. Qiu, *J. Photochem. Photobiol. C* **20**, 33 (2014)
22. Y. Han, J.Q. Di, A.D. Zhao, Z.H. Zhang, *Appl. Organomet. Chem.* **33**, 5172 (2019)
23. N. Azizi, T. Soleymani Ahoovie, M. Mahmodi Hashemi, I. Yavari, *Synlett* **29** 645 (2018)
24. Y.R. Du, B.H. Xu, J.S. Pan, Y.W. Wu, X.M. Peng, Y.F. Wang, S.J. Zhang, *Green Chem.* **21**, 4792 (2019)
25. S. Sun, S. Liang, *Nanoscale* **9**, 10544 (2017)
26. G. Mamba, A.K. Mishra, *Appl. Catal. B* **198**, 347 (2016)
27. Q. Liu, S. Yu, L. Hu, M. Ijaz Hussain, X. Zhang, Y. Xiong, *Tetrahedron* **74** 7209 (2018)
28. C. Qian, T. Huang, *J. Org. Chem.* **63**, 4125 (1998)
29. X.C. Li, S.S. Gong, D.Y. Zeng, Y.H. You, Q. Sun, *Tetrahedron Lett.* **57**, 1782 (2016)
30. G. Gao, M.N. Chen, L.P. Mo, Z.H. Zhang, *Phosphorus Sulfur Silicon Relat. Elem.* **194**, 528 (2019)
31. M. Nazish, S. Mohd, N.U.H. Khan, P. Kumari, R.I. Kureshy, S.H.R. Abdi, H.C. Bajaj, *ChemPlusChem* **79**, 1753 (2014)
32. A.R. de Oliveira, R. Katla, M.P. Rocha, T.B. Albuquerque, C.D. da Silva, V.L. Kupfer, A.W. Rinaldi, N.L. Domingues, *Campos Synth.* **48**, 4489 (2016)
33. M. Rostamzadeh, M.T. Maghsoodlou, N. Hazeri, S.M. Habibi-khorassani, L. Keishams, *Phosphorus Sulfur Silicon Relat. Elem.* **186**, 334 (2011)
34. P. Lee, K. Lee, *Chem. Commun.* **17**, 1698 (2001)
35. N. Azizi, M.R. Saidi, *Tetrahedron* **59**, 5329 (2003)
36. G.Y. Sun, J.T. Hou, J.J. Dou, J. Lu, Y.J. Hou, T. Xue, Z.H. Zhang, *J. Chin. Chem. Soc.* **57**, 1315 (2014)
37. S. Bhagat, A.K. Chakraborti, *J. Org. Chem.* **72**, 1263 (2007)
38. S. Bhagat, A.K. Chakraborti, *J. Org. Chem.* **73**, 6029 (2008)
39. G. Keglevich, V. Róza Tóth, L. Drahos, *Heteroat. Chem.* **22**: 15 (2011)
40. G. Laven, M. Kalek, M. Jezowska, J. Stawinski, *New J. Chem.* **34**, 967 (2010)
41. B. Iorga, F. Eymery, P. Savignac, *Tetrahedron Lett.* **39**, 3693 (1998)
42. T. Soleymani Ahoovie, N. Azizi, M. Mahmoudi Hashemi, I. Yavari, *Res. Chem. Intermed.* **44**, 1425 (2018)
43. N. Azizi, M. Mariami, M. Edrisi, *Dyes Pigm.* **100**, 215 (2014)

44. N. Azizi, S. Dezfooli, M.M. Hashemi, *Comptes Rendus Chim.* **16**, 997 (2013)
45. N. Azizi, T.S. Ahoie, M.M. Hashemi, *J. Mol. Liq.* **246**, 221 (2017)
46. N. Azizi, E. Gholibeghlo, Z. Manocheri, *Sci. Iranica* **19**, 574 (2012)
47. E. Mollashahi, H. Gholami, M. Kangani, M. Lashkari, M.T. Maghsoodlou, *Heteroat. Chem.* **5**, 322 (2015)

Publisher's Note Springer Nature remains neutral with regard to jurisdictional claims in published maps and institutional affiliations.